Journal of Environmental Management 191 (2017) 189–197

Contents lists available at ScienceDirect

Journal of Environmental Management

journal homepage: www.elsevier.com/locate/jenvman

Research article

Coagulation-flocculation sequential with Fenton or Photo-Fenton processes as an alternative for the industrial textile wastewater treatment

Edison GilPavas [a, *], Izabela Dobrosz-Gómez [b], Miguel Ángel Gómez-García [c]

[a] GIPAB: Grupo de Investigación en Procesos Ambientales, Departamento de Ingeniería de Procesos, Universidad EAFIT, Carrera 49 #7 sur 50, Medellín, Colombia

[b] Grupo de Investigación en Procesos Reactivos Intensificados con Separación y Materiales Avanzados - PRISMA, Departamento de Física y Química, Facultad de Ciencias Exactas y Naturales, Sede Manizales, Campus La Nubia, Km 9 Vía al Aeropuerto la Nubia, Apartado Aéreo 127, Manizales, Caldas, Colombia

[c] Grupo de Investigación en Procesos Reactivos Intensificados con Separación y Materiales Avanzados - PRISMA, Departamento de Ingeniería Química, Facultad de Ingeniería y Arquitectura, Universidad Nacional de Colombia, Sede Manizales, Campus La Nubia, Km 9 Vía al Aeropuerto la Nubia, Apartado Aéreo 127, Manizales, Caldas, Colombia

ARTICLE INFO

Article history:
Received 20 July 2016
Received in revised form
29 December 2016
Accepted 7 January 2017
Available online 14 January 2017

Keywords:
Advanced oxidation processes
Chemical coagulation
Fenton
Photo-Fenton
Industrial textile wastewater

ABSTRACT

In this study, the industrial textile wastewater was treated using a chemical-based technique (coagulation-flocculation, C-F) sequential with an advanced oxidation process (AOP: Fenton or Photo-Fenton). During the C-F, $Al_2(SO_4)_3$ was used as coagulant and its optimal dose was determined using the jar test. The following operational conditions of C-F, maximizing the organic matter removal, were determined: 700 mg/L of $Al_2(SO_4)_3$ at pH = 9.96. Thus, the C-F allowed to remove 98% of turbidity, 48% of Chemical Oxygen Demand (COD), and let to increase in the BOD_5/COD ratio from 0.137 to 0.212. Subsequently, the C-F effluent was treated using each of AOPs. Their performances were optimized by the Response Surface Methodology (RSM) coupled with a Box-Behnken experimental design (BBD). The following optimal conditions of both Fenton (Fe^{2+}/H_2O_2) and Photo-Fenton (Fe^{2+}/H_2O_2/UV) processes were found: Fe^{2+} concentration = 1 mM, H_2O_2 dose = 2 mL/L (19.6 mM), and pH = 3. The combination of C-F pretreatment with the Fenton reagent, at optimized conditions, let to remove 74% of COD during 90 min of the process. The C-F sequential with Photo-Fenton process let to reach 87% of COD removal, in the same time. Moreover, the BOD_5/COD ratio increased from 0.212 to 0.68 and from 0.212 to 0.74 using Fenton and Photo-Fenton processes, respectively. Thus, the enhancement of biodegradability with the physico-chemical treatment was proved. The depletion of H_2O_2 was monitored during kinetic study. Strategies for improving the reaction efficiency, based on the H_2O_2 evolution, were also tested.

1. Introduction

The textile industry uses a great amount of chemical compounds during its production processes. Among them, dyes, detergents, waxes, surfactants, solvents, salts, and other organic compounds can be mentioned. As a consequence, textile wastewater contains high loading of organic pollutants, which represents high values of Chemical Oxygen Demand (COD) and Total Organic Carbon (TOC), as well as low biodegradability, expressed as a low ratio between the Biochemical Oxygen Demand (BOD_5) and COD (BOD_5/COD) (Lapertot et al., 2007; Rodriguez et al., 2002). It implies that a chemical treatment is required before the wastewater will be discharged into the environment or into a biological treatment plant (Punzi et al., 2015; Soares et al., 2015; Araña et al., 2013).

Degradation of recalcitrant pollutants can be achieved by Advanced Oxidation Processes (AOPs), among them Fenton (FT) and Photo-Fenton (PF) ones. They were found to be an alternative for treating a wide range of contaminants (Brillas and Martínez-Huitle, 2015). The non-biodegradable pollutants such as: herbicides (González et al., 2014) landfill leachate (He et al., 2015) and wastewater coming from textile industries (Rodríguez-Chueca et al., 2016; Soares et al., 2013; Byberg et al., 2013; Nidheesh

* Corresponding author.
E-mail address: egil@eafit.edu.co (E. GilPavas).

http://dx.doi.org/10.1016/j.jenvman.2017.01.015
0301-4797/

et al.,2013; GilPavas et al., 2012), have already been successfully treated. The AOPs are based on the generation of non-selective and highly oxidative reactive species, mainly the hydroxyl radicals (•OH), responsible for organic substrate oxidation (2.8 V vs. NHE) in the Fenton reactions (Vedrenne et al., 2012).

The FT process is one of the most studied AOPs, due to its efficiency, low reaction time, and easy application (Pignatello et al., 2006). Here, the •OH radical and reactive oxidizing species are produced by the catalytic decomposition of H_2O_2 with iron. The Fenton reaction mechanism is well known. The Fe^{+3} ion, dissolved in water, is subjected to form different complexes; for instance, at pH close to 3, $[Fe(H_2O)_5(OH)]^{2+}$ become the predominant stable species. It is also possible to use solar radiation to promote the generation of Fe^{2+} ions, increasing the •OH radical production rate and enhancing the efficiency of the process. It is denominated the PF reaction, and occurs according to Eqs. (1)–(3) (Malato et al., 2009).

$$Fe^{2+} + 6H_2O \rightarrow [Fe(H_2O)_6]^{2+} \quad (1)$$

$$[Fe(H_2O)_6]^{2+} + HO^- \rightarrow [Fe(H_2O)_5(OH)]^{+} + H_2O \quad (2)$$

$$[Fe(H_2O)_5(OH)]^{+} + h\nu \rightarrow Fe^{2+} + 5H^{+} + 6HO^{\bullet} \quad (3)$$

The conventional treatment for textile wastewater consists of a coagulation-flocculation (C-F) process followed by sand filtration (Amor et al., 2015). However, it is only able to remove suspended solids, whereas soluble organic compounds remain unaffected. This implies the necessity of introducing a subsequent treatment step. Thus, coagulation is an effective "pre-treatment" process. The coupling of C-F with the FT process can be an appropriate alternative to achieve high levels of wastewater decontamination (Li et al., 2016; García-Montaño et al., 2006). Moreover, since solution transmittance improves after solids removal, photo-induced processes (*v.g.*, PF) become a potential alternative for "final" wastewater treatment.

The C-F processes for the treatment of textile wastewater have been extensively studied (Verma et al., 2012; Khouni et al., 2011; Kwang-Ho et al., 2007). It is essential to reduce total suspended solids, organic content, and color in order to improve later treatment's efficiency (Amor et al., 2015). Aluminum salts are the most widely used coagulants. They let to achieve *ca.* 50–60% of COD, and 90–100% of suspended solids removal. Besides, they are widely available and cheap, comparing to the other coagulants. Aluminum salts acidifies the solution during coagulation. This is a useful characteristic for coupling C-F with Fenton processes which are known to work best around pH values of 3 (Khouni et al., 2011; Malato et al., 2009; Kwang-Ho et al., 2007).

Recently, few authors have reported on the C-F sequential with FT or PT process for the treatment of industrial wastewater (Li et al., 2016; Senn et al., 2014; Perdigón-Melón et al., 2010). The sequential technologies improves synergetically the efficiency of Fenton process. It was reported that lower amounts of iron load and lower operation time are needed for the treatment of wastewaters using a PF process; decreasing the operational costs considerably. Additionally, the PF process driven by natural UV can be considered an environmentally friendly technology as it generates low to zero waste and prevents pollution. Unfortunately, the most of these studies, operational conditions are case specific and need to be rigorously optimized. As far as we know, any statistical methods were applied to investigate systematically the combination of parameters that provides optimal conditions of both the FT and PF processes combined with C-F for the treatment of industrial textile wastewater.

Thus, this work presents the application of sequential C-F-Fenton (C-F-FT) and C-F-Photo Fenton (C-F-PF) processes for the treatment of textile effluents from an industrial facility located in Medellín (Colombia). At first, a complete characterization of the wastewater effluent was made in terms of its biodegradability (BOD_5/COD), organic matter loading (TOC, COD, BOD_5), and solids content (total solids and turbidity). Secondly, the potential of a sequential C-F-FT and C-F-PF process was evaluated. For this purpose, initially the C-F process was optimized using the jar test methodology. Then, the Response Surface Methodology (RSM) coupled with Box-Behnken experimental design (BBD) was performed to optimize the FT and PF processes, in terms of the organic matter degradation efficiency. The advantage of these optimization methods relies on the reduction of the number of experimental trials, in comparison with the complete factorial designs. They allow to develop the mathematical models for the assessment of the statistical significance of each variable and their interactions (GilPavas et al., 2014; El-Ghenymy et al., 2012). Finally, the depletion of H_2O_2 was monitored during kinetic study. Some strategies for improving the reaction efficiency, based on the H_2O_2 consumed, were also tested.

2. Materials and methods

2.1. Wastewater samples

The wastewater samples were collected from an equalization tank of an industrial textile plant located in Medellín (Colombia). They showed a dark blue color associated with the mixture of several classes of dyes (Reactive, Direct, Dispersive, Acid and Cuba dyes) as well as other pollutants used in the textile process. The samples were kept refrigerated in order to avoid compounds degradation during storage and transportation, following the standard procedures (Eaton et al., 2005). They present an intensive blue color, mainly due to the presence of indigo dye, which represents a high percentage of organic compounds in the wastewater. The characteristics of the industrial wastewater and the Colombian permissible limits for the industrial wastewater discharges are summarized in Table 1.

Several physico-chemical parameters of the analyzed industrial wastewater present values beyond the emission limit range (e.g., pH, COD, and TS). It is characterized with high-conductivity due to the presence of different salts. Moreover, it shows a high COD value, more than twice of that of the permissible limit. This implies the presence of large amount of non-biodegradable organic matter. In fact, the initial BOD_5/COD ratio, equaled to *ca.* 0.14 (<0.35), indicates that the analyzed effluent is not biodegradable (Lapertot

Table 1
Physico-chemical characterization of the industrial textile wastewater stream and the permitted discharge limits.

Parameter	pH	Conductivity (μS/cm)	Turbidity (NTU)	COD (mg O_2/L)	TOC (mg C/L)	BOD_5 (mg O_2/L)	TS (mg/L)	AC (mg Pt/L)	BOD_5/COD
Value	9.96	4010	184	865	290	118	2464	1.274	0.1364
Permissible Limit [a]	6–9	–	–	400	–	200	50	–	–

[a] Emission limit values for industrial wastewater discharges into the municipal sewer system according to Res 0631, 17/03/2015, issued by the Ministry of Environment and Sustainable Development, Colombia. *TS: Total solids, AC: Apparent color.

et al., 2007; Rodriguez et al., 2002). Although the legally permissible limit for organic compounds is usually expressed in the terms of COD, in this study the TOC evolution was also monitored. This technique is faster and gives a direct measurement of carbon content without interference with other oxidizable inorganic substances present in the wastewater.

2.2. Reagents

All reagents were obtained from Merck and used as received without any further purification. Ferrous sulfate hepta-hydrate ($FeSO_4.7H_2O$, 99.98% purity) and hydrogen peroxide (H_2O_2, 30 wt %) were used as Fenton reagents. All solutions were prepared using ultra-pure water (Milli-Q system; conductivity < 1 μS cm^{-1}). Sample pH was adjusted using H_2SO_4 (99.1%). MnO_2 (reagent grade ≥ 90%, Sigma Aldrich) was used to quench the hydroxyl radicals action and inactivate H_2O_2 before analyses. Aluminum sulfate ($Al_2(SO_4)_3.18H_2O$) was used for the coagulation/flocculation process.

2.3. Analytical methods

Samples resulting from the laboratory tests were analyzed in triplicate using a UV–VIS double-beam spectrophotometer (Spectronic Genesys 2 PC) in the range of 200–700 nm, with a 1 cm path length quartz cell. Standard methods were used for the quantitative analysis of COD, TOC, BOD_5, TS, AC, and turbidity (Eaton et al., 2005). The COD analyses were performed following the closed reflux method with colorimetric determination (method 5220D). The TOC measurements were carried out following the method 5310D; and the BOD_5 ones, following the respirometric method (5210B). The turbidity was determined with an Orbeco-Hellige Turbidimeter (Model 966-01), following the 2130B standard method. The 2540D standard method was employed for TS measurements. Finally, H_2O_2 concentration was measured by iodometric titration with KI and $Na_2S_2O_3$. To avoid the interference of H_2O_2 during COD measurements, the residual H_2O_2 was quenched using MnO_2.

In all cases, the average value of the measurements is reported. The variability of data are presented graphically by error bars (indicating the error or uncertainty in a reported measurement).

2.4. Coagulation-flocculation pre-treatment

The operational conditions of C-F pre-treatment were determined using a laboratory jar test apparatus (Centricol Ltda). Aluminium stock solution was prepared using $Al_2(SO_4)_3 \cdot 18H_2O$. Five different concentrations were used to define the coagulant dose: 200, 400, 500, 600, and 700 mg/L. Jar tests were performed according to the standard procedure (ASTM D2035:2008). It consists of three steps: (i) a period of fast mixing (at 150 rpm) of wastewater solution with $Al_2(SO_4)_3 \cdot 18H_2O$ for 2 min; (ii), a period of slow mixing (at 20 rpm) for 20 min to induce the flocs' formation; and, (iii), 15 min of sedimentation without agitation. After completing the C-F process, the turbidity and COD, measured to the supernatant, were used as response variables to determine the coagulant dose. The supernatant obtained at the most effective conditions was separated to evaluate the efficiency of the C-F-FT and C-F-PF processes.

2.5. Reaction system

The FT reaction was carried out in a continuously stirred glass reactor with 80 mL total volume. The PF process used a 150 mL cylindrical quartz reactor, with an internal hole where a lamp of UV radiation was introduced. A black-light tubular lamp (maximum light intensity at λ = 365 nm, 15 mm of diameter, 225 mm of length, model F6T5/BL Philips, 6 W, photon flux of $1.47*10^{19}$ $1/m^2/s$, radiant flux of 0.5 mW/cm^2) was used. The radiation flux was measured using a radiometer Delta Ohm HD 2102 and the total irradiated area was of 100 cm^2. The reaction time was fixed at 45 min. In all experiments, the solution was stirred (140 rpm) with a magnetic bar to ensure its homogenization and to avoid mass transfer effects. The schemas of the experimental set-ups are included in the supplementary material.

2.6. Statistical model and experimental design

The RSM was employed to establish the effect of different operational conditions on the FT and PF performance for wastewater treatment. Several operational factors have been found to affect the efficiency of both processes. The effect of pH have already been widely studied (De Laat et al., 2011). Indeed, it is well known that iron tends to form insoluble aqua complexes at pH above 4, losing its catalytic capacity (Papoutsakis et al., 2015). However, some authors have successfully performed the Fenton reaction near neutral pH (Miralles-Cuevas et al., 2014; Moncayo-Lasso et al., 2008). The concentration of Fenton reagents (*v.g.*, Fe^{2+} and H_2O_2) also affects directly the efficiency of the process and optimal conditions, depending on the nature and pollutants concentration (Malato et al., 2009). In this work, the pH, Fe^{2+} and H_2O_2 concentrations were chosen as independent variables (operational factors). Their levels were chosen from our previous work (GilPavas et al., 2015). They were evaluated in the following ranges: pH = 3–6; Fe^{2+} concentration = 0.25–1.25 mM; and H_2O_2 dose = 1–10 mL/L (9.8–98 mM). Other variables, such as initial pollutant concentration and conductivity, were fixed at natural conditions of the wastewater.

A multifactorial BBD was defined in order to establish the synergetic effects of the operational factors and to optimize their conditions (i.e., to maximize the organic matter degradation) (Secula et al., 2014). The BBD allows: (i) to estimate the parameters of the quadratic model; (ii) to build the sequential experimental designs; (iii) to detect the lack of fitting of the model; and (iv) to use the blocks. It is important to clarify that RSM was not used to understand the wastewater degradation mechanism but to determine the optimal operational conditions at certain operating specifications. Regression coefficients and their effects were analyzed using the analysis of variance (ANOVA), including the use of Pareto diagram and *p*-values (at probability levels lower than 0.05). Table 2 present the operational factor at the evaluated levels.

The proposed BBD, involving three independent variables (factors), required 15 experiments (including three central points). All essays were carried out in duplicates. The average value of each measurement was used for data analysis. The response variable, to assess the process efficiency, was the percentage of COD degradation (%DCOD). It was calculated according to Eq. (4).

$$\%DCOD = \frac{COD_0 - COD_F}{COD_0} * 100 \quad (4)$$

Table 2
Variables (factors) and their levels for BBD.

Variables	Coded factors, X		
	−1 Level 1	0 Level 2	1 Level 3
H_2O_2 (mL/L)	1 (9.8 mM)	5.5 (54 mM)	10 (98 mM)
Fe^{2+} (mM)	0.25	0.75	1.25
pH	3	4.5	6

Table 3
Residual turbidity for different coagulant dosage.

$Al_2(SO_4)_3 \cdot 18H_2O$ (mg/L)	200	400	500	600	700	800
COD (mg O_2/L)	806	698	615	566	450	456
Residual turbidity (NTU)	173	96	13	11	3	4

For the RSM, the experimental results were adjusted to a second-order multi-variable polynomial model, Eq. (5), using Statgraphics Centurion XVI Software.

$$Y_i = \beta_0 + \sum_1^3 \beta_i x_i + \sum_1^3 \beta_{ii} x_{ii}^2 + \sum_1^3 \sum_1^3 \beta_{ij}\, x_i x_j \quad (5)$$

where β_0, β_i, β_{ii}, and β_{ij} are the regression coefficients for the intercept, linear, square, and interaction terms, respectively; and x_i and x_j are independent variables. The quality of the model and its prediction capacity were judged from the variation coefficient, R^2. From the developed mathematical model, the individual and synergetic effects of the operating factors on the response variables, using three-dimensional response surface plots, were mapped. Details of this methodology have already been reported elsewhere (GilPavas et al., 2015, 2016; Ghanbari and Moradi, 2015).

3. Results and discussion

3.1. Textile wastewater pre-treatment by coagulation-flocculation

The evolution of COD and residual turbidity using different coagulant concentrations are presented in Table 3.

The significant improvement in wastewater quality, equivalent to 48% of COD, 100% of color and 98.37% of turbidity removal, was observed at 700 mg/L of $Al_2(SO_4)_3 \cdot 18H_2O$ dosage. It was defined as the working coagulant concentration. At these conditions, the characterization of the C-F supernatant was performed. The obtained results are compared to the original values in Table 4. The C-F process was able to reduce organic loading. However, it failed to achieve COD discharge limits. Although the pre-treatment eliminates (almost completely) the wastewater turbidity, it was inefficient in removing surfactants and other soluble organic pollutants present in the sample. Thus, it was possible to remove only 48% and 16% of COD and TOC, respectively. The biodegradability ratio BOD_5/COD increased slightly from 0.136 to 0.212, still being very low value (<0.35). Therefore, a biological treatment cannot be adequate to degrade these residual pollutants and physicochemical treatment is required. It is important to notice that after the C-F, the effluent pH decreased from 9.96 to 6. Thus, this last value was chosen as the superior limit of pH to evaluate the efficiency of the FT and PF processes.

3.2. Fenton and Photo-Fenton processes

In order to reduce the concentration of COD and to increase the biodegradability of the effluent resulting from the C-F process, FT and PF oxidation processes were applied. In this sense, RSM analysis was used independently for both processes in order to determine the individual and interactive effects of the operating variables for each treatment.

3.2.1. Box-Behnken experimental design and optimization model

The experimental design (conditions) for both FT and PF processes, together with the obtained results, are given in Table S1 (see supplementary material). The observed COD removal percentages varied between *ca.* 12 and 37% for the FT process and from 14 to 78% for the PF process. The most efficient experimental conditions were the same for both processes: pH = 3, Fe^{2+} concentration = 0.75 mM, and [H_2O_2] dose = 10 mL/L (98 mM). However, the efficiency was always considerably higher using the PF process.

For both FT and PF processes, %DCOD data were adjusted to the second order polynomial model, as described in Eq. (5). The empirical models, equations (6) and (7), represent the %DCOD as a function of three independent process variables (H_2O_2 dose, Fe^{2+} concentration, and pH). They describe how %DCOD was affected by the individual variables and/or their double interactions. Thus, % DCOD was linear and also quadratic with respect to all three analyzed variables.

$$\begin{aligned} \%DCOD\ FT = {} & 50.115 + (1.30957{*}H_2O_2) + \left(32.8139{*}Fe^{2+}\right) \\ & - (19.4806{*}pH) - \left(0.0339506{*}(H_2O_2)^2\right) \\ & - \left(0.588889{*}H_2O_2{*}Fe^{2+}\right) \\ & - (0.0111111{*}H_2O_2{*}pH) - \left(5.35{*}\left(Fe^{2+}\right)^2\right) \\ & - \left(2.36667{*}Fe^{2+}{*}pH\right) + \left(2.16111{*}(pH)^2\right) \end{aligned} \quad (6)$$

$$\begin{aligned} \%DCOD\ PF = {} & 117.575 + (4.39208{*}H_2O_2) + \left(99.875{*}Fe^{2+}\right) \\ & - (55.5509{*}pH) - \left(0.0687243{*}(H_2O_2)^2\right) \\ & - \left(0.1{*}H_2O_2{*}Fe^{2+}\right) - (0.640741{*}H_2O_2{*}pH) \\ & - \left(10.2667{*}\left(Fe^{2+}\right)^2\right) - \left(13.0667{*}Fe^{2+}{*}pH\right) \\ & + \left(6.41481{*}(pH)^2\right) \end{aligned} \quad (7)$$

3.2.2. Analysis of variance and statistical significance

The ANOVA was used to determine the significant main and interaction effects of factors influencing %DCOD. It consists of

Table 4
The effect of C-F pre-treatment on physico-chemical characterizationof studied textile effluent.

Parameter	Initial wastewater sample	Coagulation-flocculation supernatant
pH	9.96	6
Conductivity (μS/cm)	4010	4500
Turbidity (NTU)	184	3
COD (mg O_2/L)	865	450
TOC (mg C/L)	290	151
BOD_5 (mg O_2/L)	118	96.5
BOD_5/COD	0.136	0.212
Generated sludge (kg/m^3)	–	0.472

classifying and cross-classifying statistical results, decomposing the contribution of each variable (or factors) and their double-interactions in the variance of each response variable (%DCOD). The inclusion of double-interaction and self-double-effect implies that changes in the response variable cannot be explained by independent effects. Rather, the explanation infers more complicated relationships among variables. The *p*-values were used to identify experimental parameters that present statistical influence on particular response. If *p*-value is lower than 0.05, it is considered that the specific variable shows statistical significance within the 95% confidence level (Montgomery, 2010). Table 5 presents a summary of the ANOVA results for each of the response variables and the values of probability (*p*-values). Notice that, for both FT and PF processes, the *p*-values of pH and Fe^{2+} concentration were lower than 0.05. Therefore, they are considered as statistically relevant in the degradation process. Indeed, the pH effect on the reaction performance can be attributed to the stability of the iron complexes in the solution (Miralles-Cuevas et al., 2014). The H_2O_2 concentration resulted to be insignificant for either the FT or PF processes, in the evaluated experimental range. Several studies have concluded that too low H_2O_2 concentration leads to the reduction of Fenton reaction rate, while too high concentration may induce H_2O_2 competition for $^{\bullet}OH$ radicals. Usually, there is a rather broad H_2O_2 concentration interval between both extremes, where none of both phenomena occurs (Byberg et al., 2013). It is quite remarkable that the interaction between Fe^{2+} concentration and pH resulted statistically significant in the PF process. Such effect on the response variable will be discussed in a subsequent section.

The quality of the fitted model, concerning its capacity to predict properly the response variable, was evaluated based on the determination coefficients, R^2 and R^2_{adj} (Table 5). Their values indicate that Eqs (6) and (7) explain *ca.* 94% of the variability observed in the COD degradation data for both FT and PF process. The R^2_{adj} is a more rigorous parameter to determine the quality of the models. Likewise, the obtained model can explain *ca.* 85% of the variability observed in the experimental data.

The Pareto diagram illustrates the statistical significance of each factor and its interactions. It represents graphically the standardized effects, from the highest to the lowest one in magnitude. Its sign indicates if an increase in the level of the factor presents a positive (+) or negative (−) effect on the response variable. Fig. 1 presents the Pareto diagram for the %DCOD using FT and PF process. A Pareto diagram is a series of bars whose heights (b_i) reflect the frequency or impact of each factor. The bars are arranged in descending order of heights from left to right. Therefore, the factors represented by the tall bars are relatively more significant. Here, the Pareto analysis was also carried out to determine the percentage effect of each factor (P_i) according to Eq. (8).

$$P_i = \left[\frac{b_i^2}{\sum b_i^2}\right] * 100 \quad (i \neq 0) \tag{8}$$

For the FT process, the factor with the greatest effect on the % DCOD was the Fe^{2+} concentration, accounting *ca.* 52% of the total effects. Its positive sign indicates that the highest degradation efficiency was obtained at the highest levels of this factor. This is consistent with the most of results presented in the open literature where an increase in iron concentration (equal or less than 1 mM) always let to an increase in reaction rate (Gernjak et al., 2006). The Fe^{2+} concentration induces a similar effect on the PF process, accounting *ca.* 26% of the total effects. The pH value presents an inverse proportional effect on both the FT and PF processes. In fact, higher degradation efficiencies were obtained at the lowest pH levels in the evaluated pH range. This result is also consistent with many other experimental results. Actually, for Fenton processes, it has been widely accepted that the optimal pH is between 2.8 and 3 (Kavitha and Ppanalivelu, 2005). At such conditions, iron precipitation is avoided when it is used at concentrations near to 1 mM. For the PF reaction, the pH was the factor with the highest effect over the %DCOD. It could be attributed to the formation of iron complexes, at pH near 3, which can absorb UV radiation more efficiently and let to increase in the degradation rate (Parra et al., 2000). The H_2O_2 dosage resulted to present a slightly positive effect on the %DCOD, in the evaluated range (9.8–98 mM), meaning that degradation reaction takes place successfully at low H_2O_2 concentration (increasing its dosage produce only a slight efficiency increase).

Table 5
The ANOVA for %DCOD as a function of H_2O_2 dosage (A), Fe^{2+} concentration (B), and pH (C), according to the BBD.

Variables and interactions	*p-value*	
	%DCOD - FT	%DCOD - PF
A:H_2O_2	0.0564	0.3074
B:Fe^{2+}	0.0011	0.0054
C:pH	0.0180	0.0016
AA	0.5888	0.7390
AB	0.2993	0.9550
AC	0.9503	0.3062
BB	0.3125	0.5446
BC	0.1816	0.0493
CC	0.0095	0.0147
Model Fit		
R^2 (%)	94.54	94.42
R^2_{adj} (%)	84.71	84.36

3.2.3. Optimal conditions based on factor interaction analysis

During Fenton reactions, organic matter oxidation takes place by successive attacks of non-selective reactive oxygen species (ROS) driven by the iron mediated decomposition of H_2O_2. One can expect a straight relation between the %DCOD and ROS availability. However, in this case, the optimal conditions for Fenton processes imply both the lowest amount of reagents and the highest degradation efficiency. Statistical analysis allows finding such operational conditions. Thus, Fig. 2 presents the factor interaction plots between pH-H_2O_2 dosage and pH–Fe^{2+} concentration for FT and PT processes. In all cases, the %DCOD is higher at pH *ca.* 3. In fact, the formation of insoluble Fe^{3+} complexes, that inhibits Fe^{2+} regeneration necessary for the Fenton reactions, is more probable at higher pH values. One can see that at pH = 6, an increase in H_2O_2 dosage presents any significant effect on %DCOD. Indeed, dissolved iron becomes the limiting reagent; so, an excess of H_2O_2 or suspended iron will not have any effect in the process efficiency (Arslan-Alaton et al., 2009).

During the PF process, at pH = 3, the efficiency of COD removal was significantly higher than that observed for FT one. This due to both high solubility and high UV radiation absorption capacity of the predominant iron species ($[Fe(H_2O)_5(OH)]^{2+}$) (Malato et al., 2009; Ghaly et al., 2001). Additionally, at this pH, an increase in H_2O_2 dosage, from 1 to 10 mL/L, the COD removal improves only in 14% (from *ca.* 51 to 65 %DCOD) during 45 min (Fig. 2 (a) and (b)). It could be explained considering the inhibitory effect of excessive H_2O_2 amount (free radical scavenging), as expressed by the following reaction (Brillas and Martínez-Huitle, 2015):

$$H_2O_2 + HO^{\bullet} \rightarrow H_2O + HO_2^{\bullet} \quad k = 2.7*107\ M^{-1}s^{-1} \tag{9}$$

Therefore, low H_2O_2 concentrations are preferred in order to minimize reactant consumption. Moreover, as evidenced in Fig. 2 (c) and (d), an increase in Fe^{2+} concentration improved the

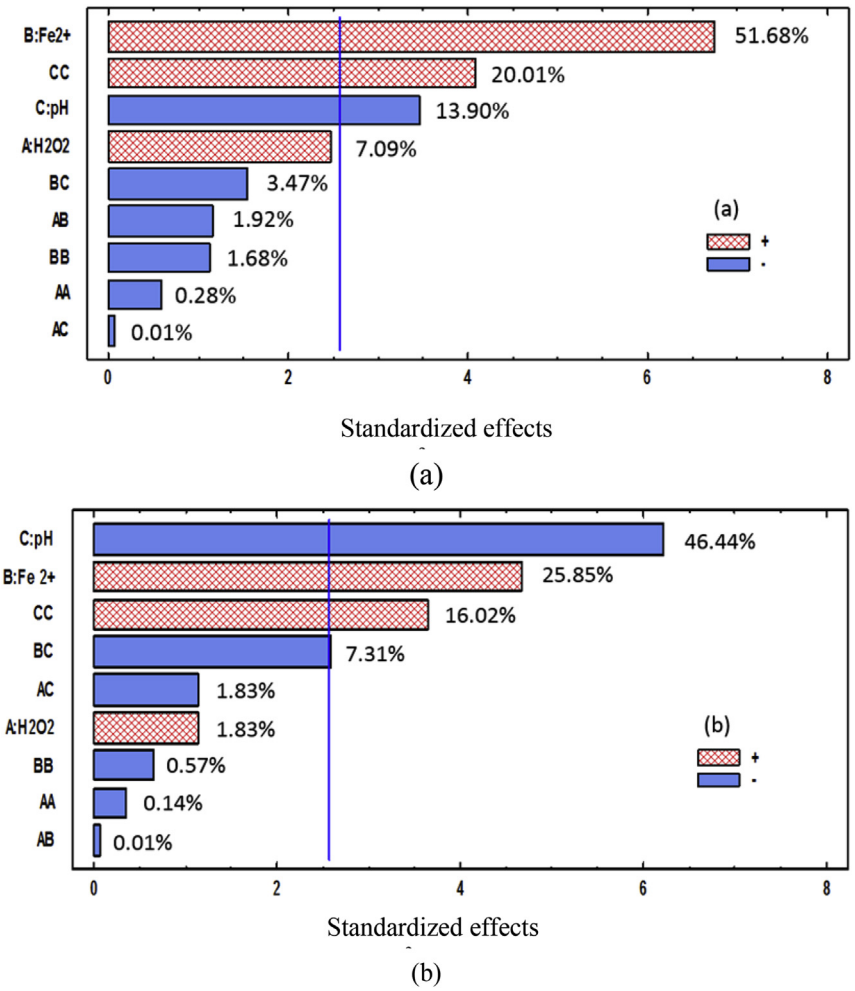

Fig. 1. Pareto diagram for the %DCOD using FT (a) and PF (b) process.

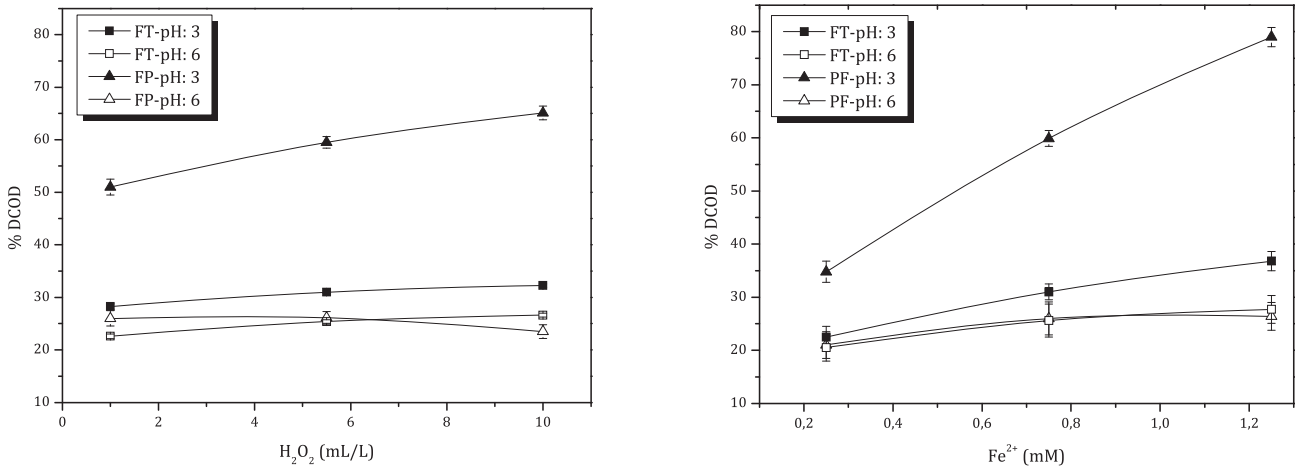

Fig. 2. The pH − H_2O_2 dosage and the pH − Fe^{2+} concentration interaction plots, for FT and PF processes, obtained for %DCOD.

efficiency of COD. Under low iron concentrations, H_2O_2 is consumed by less desirable reactions, while part of H_2O_2 is decomposed into molecular oxygen and water, without the generation of HO•. In the presence of high iron concentrations, the process is accelerated due to the regeneration of Fe^{2+} from Fe^{3+} reduction, resulting in the rapid and additional generation of HO• radicals (Zapata et al., 2009).

Response surface plots are considered as useful tools to observe the simultaneous effects of two factors over a response variable. Fig. 3 (a) and (b) show them for FT and PF processes, respectively. They were constructed from the polynomial models described by Eqs (6) and (7), for a fixed pH value of 3. As it can be seen the

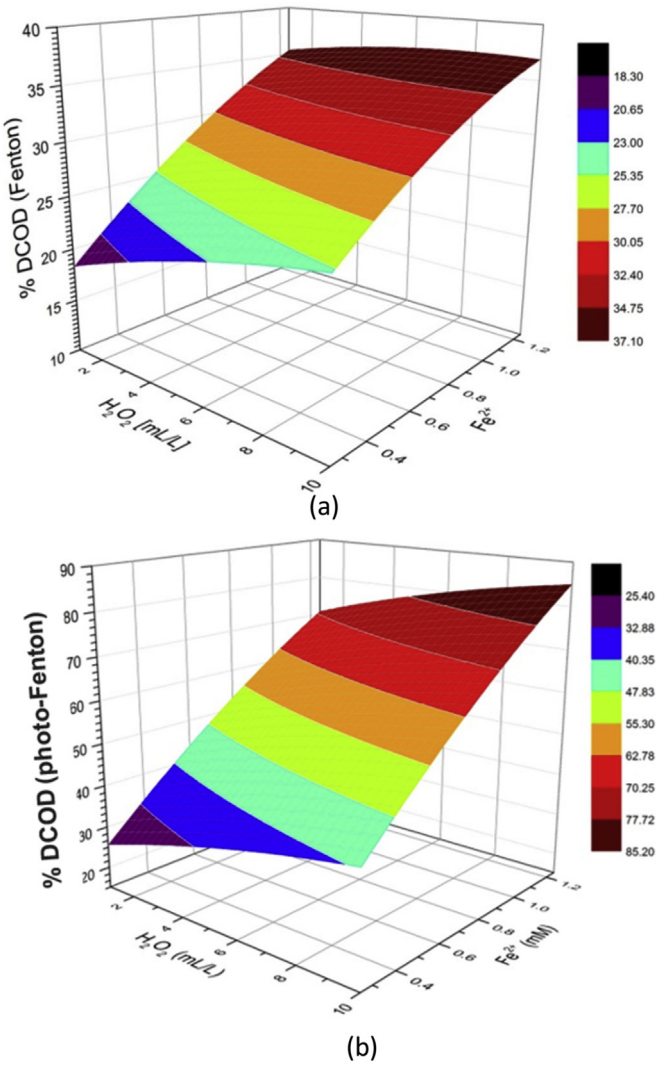

Fig. 3. Response surface diagrams for the interactive effect of H_2O_2 dosage and Fe^{2+} concentration on %DCOD for FT (a) and PF (b) processes (reaction time = 45 min, temperature = 25 °C, pH = 3).

application of the highest Fe^{2+} concentration let to achieve the highest %DCOD, reaching *ca.* 80% for the PF process, if both of the independent parameters (H_2O_2 amount and Fe^{2+} concentration) were kept at their maximum values. Thus, considering the results of the statistical analysis and the interest in minimizing the reactant consumption, the following conditions were selected to study the evolution of the reaction with time: pH = 3, Fe^{2+} concentration = 1 mM, and H_2O_2 concentration = 2 mL/L (19.6 mM).

3.2.4. The evolution of %DTOC and H_2O_2 consumption during the FT and PF processes

Fig. 4 presents the %DTOC, as a function of time, for the FT and PF processes (lines serves as a guide to the eye). The TOC is the amount of carbon found in an organic compound and is often used as a non-specific indicator of water quality. As the oxidation advances, the organic molecules are oxidized into CO_2, leading to the TOC reduction (He et al., 2015). Consequently, the percentage of TOC depletion (%DTOC) is a measurement of the level of mineralization reached by the proposed process. One can see that both processes present comparable reaction rate during first 15 min. However, the

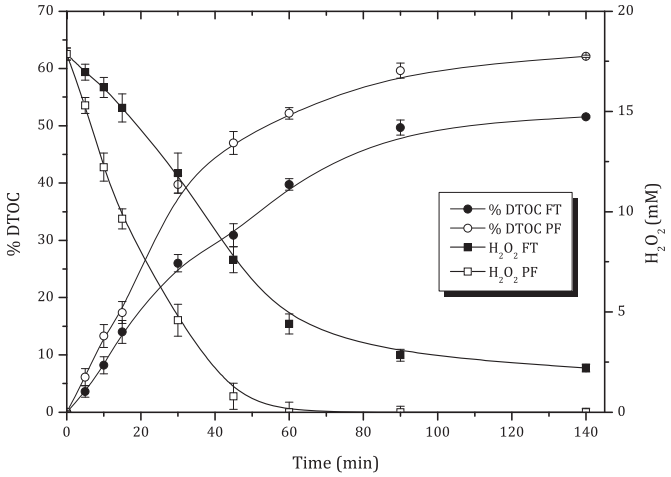

Fig. 4. The %DTOC and H_2O_2 depletion using the FT and PF processes (pH = 3, Fe^{2+} concentration = 1 mM, H_2O_2 dosage = 2 mL/L (19.6 mM)).

PF process rapidly exceeds the capacity of the FT one, reaching *ca.* 60 %DTOC after 140 min of reaction. The higher efficiency of the PF process is attributed to the faster Fe^{2+} regeneration, catalyzed by the incident radiation (Carra et al., 2014). The H_2O_2 consumption also indicates that its catalytic decomposition is much faster when the process is UV intensified (Fig. 4). In fact, after *ca.* 60 min of PF reaction, H_2O_2 concentration is below detectable limits; while for the FT process, it remains in *ca.* 20% of its initial amount. Notice also that during the PF process, after H_2O_2 depletion, the mineralization rate slowed down sharply until stabilization. This behavior has also been reported by different authors (Georgi et al., 2007; Du et al., 2006) and suggests that the degradation efficiency can be enhanced by H_2O_2 re-injection or dosage strategies.

3.2.5. Evolution of %DCOD with H_2O_2 re-injection and dosage strategies

Basing on the changes in H_2O_2 amount with time (Fig. 4), two strategies (with equaled total amounts of H_2O_2) were evaluated with the purpose of increasing in the efficiency of the PF process:

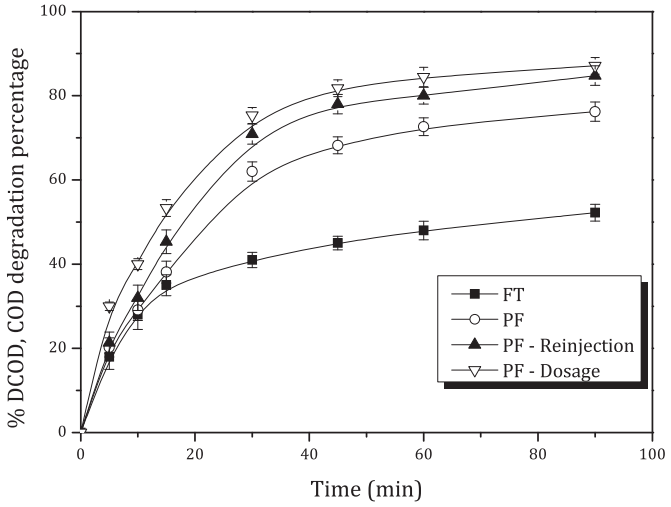

Fig. 5. The comparison of COD removal efficiency with time using FT and PF processes with these obtained using H_2O_2 re-injection and dosage strategies (pH = 3, Fe^{2+} concentration = 1 mM). The wastewater was pre-treated by C-F, removing 45% of the original COD.

Table 6
Physico-chemical characterization of the industrial textile wastewater after each step of the treatment.

Parameter	Initial Sample	Coagulation-flocculation supernatant	FT	PF	PF*
pH	9.96	6	5.31	3.64	3.7
Conductivity (μS/cm)	4010	4500	4.73	4.5	4.5
Turbidity (NTU)	184	3	5	5	5
COD (mg O_2/L)	865	450	225	112	76
TOC (mg C/L)	290	151	80	58	45
BOD_5 (mg O_2/L)	118	96.5	153	82	74
BOD_5/COD	0.14	0.21	0.68	0.74	0.97
Generated sludge (kg/m^3)	–	0.47	–	–	–

FT and PF processes running at: pH = 3, Fe^{2+} concentration = 1 mM, and H_2O_2 dosage = 19.6 mM; reaction time = 90 min * Total H_2O_2 dosage: 27 mM.

- The H_2O_2 reinjection: At the selected conditions (pH = 3, Fe^{2+} concentration = 1 mM, and H_2O_2 dose = 2 mL/L (19.6 mM) a subsequent dose of 0.76 mL/L (7.44 mM) of H_2O_2 was added after each 20 min of reaction (additional H_2O_2 dose was determined proportionally based on the value of the remaining COD);
- The H_2O_2 dosification: The total dose of 2.76 mL/L (27 mM) of H_2O_2 was added during the reaction time in the following: 1.34 mL/L (13.12 mM) at the beginning of the reaction, 0.66 mL/L (6.46 mM) after 20 min, and 0.38 mL/L (3.72 mM) in the minutes 40 and 60.

Fig. 5 compares the %DCOD removal efficiency obtained using the FT and PF processes (pH = 3, Fe^{2+} concentration = 1 mM, H_2O_2 dose = 19.6 mM) with those obtained using the PF process with the H_2O_2 dosage and re-injection strategies. As it can be seen the FT process was the least efficient, after 20 min of reaction, the degradation rate slowed down suggesting that high percentage of unreacted H_2O_2 remains in the solution, as shown in Fig. 4. Thus, the Fe^{2+} regeneration become the limiting step (Arslan-Alaton et al., 2009; Farias et al., 2009). For the PF process, both H_2O_2 dosage strategies increased the process efficiency from 75% up to *ca.* 90% of COD degradation.

3.2.6. Biodegradability evolution and sequential treatment efficiency

The biodegradability of the discharged water into a municipal sewer system is a rough indicator of the elimination, in further wastewater treatment plants (WTPs), of potentially bio-accumulative compounds. The BOD_5/COD ratio is commonly used as a biodegradability indicator (He et al., 2015; Zapata et al., 2009). It specifies the amount of oxidizable matter that can be degraded biologically. In order to evaluate the wastewater properties and biodegradability after each step of the treatment (C-F, FT, and PF) the physico-chemical characterization of the industrial textile wastewater was carried out. The obtained results are summarized in Table 6. One can see that combining the C-F pre-treatment with the FT process let to obtain 74% of COD removal was achieved during 90 min of reaction. The C-F-PF process let to achieve 87% of COD removal in the same time. Moreover, the BOD_5/COD ratio increased from 0.21 to 0.68 and from 0.21 to 0.74 with the FT and PF processes, respectively. These results prove the enhancement of biodegradability with the physico-chemical treatment.

4. Conclusions

In this study, the industrial textile wastewater was treated using a chemical-based technique (coagulation-flocculation, C-F) sequential with an advanced oxidation process (AOP: Fenton or Photo-Fenton). The studied wastewater contained high organic loading, represented by high COD and TOC values (865 mg/L and 290 mg/L, respectively) and low degradability (BOD_5/COD ratio of 0.136). The most significant results can be summarized as follows:

- The C-F pre-treatment allow to remove *ca.* 98% of turbidity, at pH 9.8, using the $Al_2(SO_4)_3$ in the amount of 700 mg/L. It let to eliminate *ca.* 48% of COD, increasing slightly BOD_5/COD ratio from 0.136 to 0.212 (still too low to consider an effluent as biodegradable).
- The C-F effluent was subsequently treated using either Fenton or Photo-Fenton process. The following conditions, optimized using RSM-BBD technique, of both Fenton (Fe^{2+}/H_2O_2) and Photo-Fenton (Fe^{2+}/H_2O_2/UV) processes were found: Fe^{2+} concentration = 1 mM, H_2O_2 dose = 2 mL/L (19.6 mM), and pH = 3.
- The combination of C-F pre-treatment with the Fenton reagent let to remove 74% of COD during 90 min of the process, increasing the BOD_5/COD ratio from 0.212 to 0.68.
- The C-F sequential with Photo-Fenton process let to reach 87% of COD removal, in the same time, increasing the BOD_5/COD ratio from 0.212 to 0.74.
- The H_2O_2 re-injection and dosage strategies were used to improve the degradation efficiency. The addition of an extra H_2O_2 amount (7.44 mM) allowed to increase the process efficiency of *ca.* 10%.

This study showed the potential application of C-F sequential with the advanced oxidation processes for the industrial textile wastewater treatment.

Acknowledgments

The authors thank to the "Dirección de Investigación de la Universidad EAFIT, Medellín", Colombia for financial support of this research. The staff of the "Laboratorio de Ingeniería de Procesos" is also recognized for their participation.

Appendix A. Supplementary data

Supplementary data related to this article can be found at http://dx.doi.org/10.1016/j.jenvman.2017.01.015.

References

Amor, C., De Torres-Socías, E., Peres, J.A., Maldonado, M.I., Oller, I., Malato, S., Lucas, M.S., 2015. Mature landfill leachate treatment by coagulation-flocculation combined with Fenton and solar photo-Fenton processes. J. Hazard. Mater. 286, 261–268.
Araña, J., Zerbani, D., Herrera-Melian, J.A., Garzon Sousa, D., Gonzalez, O., Dona Rodriguez, J.M., 2013. Effect of additives in photocatalytic degradation of commercial azo dye Lanaset Sun Yellow 180. Photochem. Photobiol. Sci. 12, 703–708.
Arslan-Alaton, I., Tureli, G., Olmez-Hanci, T., 2009. Treatment of azo dye production wastewaters using Photo-Fenton-like advanced oxidation processes: optimization by response surface methodology. J. Photochem. Photobiol. A Chem. 202, 142–153.
Brillas, E., Martínez-Huitle, C.A., 2015. Decontamination of wastewaters containing

synthetic organic dyes by electrochemical methods. An Update. Rev. Appl. Catal. B Environ. 166–167, 603–643.
Byberg, R., Cobb, J., Martin, L.D., Thompson, R.W., Camesano, T.A., Zahraa, O., Pons, M.N., 2013. Comparison of photocatalytic degradation of dyes in relation to their structure. Environ. Sci. Pollut. Res. Res. 20, 3570–3581.
Carra, I., Malato, S., Jiménez, M., Maldonado, M.I., Sánchez, J.A., 2014. Micro-contaminant removal by solar photo-Fenton at natural pH run with sequential and continuous iron additions. Chem. Eng. J. 235, 132–140.
De Laat, J., Dao, Y.H., El Najjar, N., Hamdi, Daou C., 2011. Effect of some parameters on the rate of the catalysed decomposition of hydrogen peroxide by iron(III)-nitrilotriacetate in water. Water Res. 4, 5654–5664.
Du, Y., Zhou, M., Lei, L., 2006. Role of the intermediates in the degradation of phenolic compounds by Fenton-like process. J. Hazard. Mater. 136, 859–865.
Eaton, A., Clesceri, L., Rice, E.Y., Greenberg, A., 2005. Standard Methods for the Examination of Water and Wastewater, 20a Edición. Centenial edition. American Public Health Association (APHA), Washington.
El-Ghenymy, A., Garcia-Segura, S., Rodríguez, R.M., Brillas, E., El Begranib, M., Abdelouahid, B., 2012. Optimization of the electro-Fenton and solar photoelectro-Fenton treatments of sulfanilic acid solutions using a pre-pilot flow plant by response surface methodology. J. Hazard. Mater. 221–222, 288–297.
Farias, J., Albizzati, E.D., Alfano, O.M., 2009. Kinetic study of the photo-Fenton degradation of formic acid Combined effects of temperature and iron concentration. Catal. Today 144, 117–123.
García-Montaño, J., Doménech, X., García-Hortal, J.A., Torrades, Francesca, Peral, J., 2006. Combining photo-Fenton process with aerobic sequencing batch reactor for comercial hetero bireactive dye removal. Appl. Catal. B Environ. 67, 86–92.
Georgi, A., Schierz, A., Trommler, U., Horwitz, C.P., Collins, T.J., Kopinke, F.D., 2007. Humic acid modified Fenton reagent for enhancement of the working pH range. Appl. Catal. B Environ. 72, 26–36.
Gernjak, W., Fuerhacker, M., Fernandez-Ibañez, P., Blanco, J., Malato, S., 2006. Solar photo-Fenton treatment—process parameters and process control. Appl. Catal. B Environ. 64, 121–130.
Ghanbari, F., Moradi, M., 2015. A comparative study of electrocoagulation, electrochemical Fenton, electro-Fenton and peroxi-coagulation for decolorization of real textile wastewater: electrical energy consumption and biodegradability improvement. J. Environ.. Chem. Eng. 3, 499–506.
Ghaly, M.Y., Härtel, G., Mayer, R., Haseneder, R., 2001. Photochemical oxidation of p-chlrophenol by UV/H_2O_2 and photo-Fenton process. A comparative study. Waste Manag. 21, 41–47.
GilPavas, E., Dobrosz-Gómez, I., Gómez-García, M.Á., 2012. Decolorization and mineralization of diarylide yellow 12 (PY12) by photo-fenton process: the response surface methodology as the optimization tool. Water Sci. Technol. 65 (10), 1795.
GilPavas, E., Medina, J., Dobrosz-Gómez, I., Gómez-García, M.Á., 2014. Statistical optimization of industrial textile wastewater treatment by electrochemical methods. J. Appl. Electrochem. 44, 1421–1430.
GilPavas, E., Gómez, C.M., Rynkowski, J.M., Dobrosz-Gómez, I., Gómez-García, M.Á., 2015. Decolorization and mineralization of yellow 5 (E102) by UV/Fe^{2+}/H_2O_2 process. Optimization of the operational conditions by response surface methodology. Comptes Rendus Chim. 18, 1152–1160.
GilPavas, E., Dobrosz-Gómez, I., Gómez-García, M.Á., 2016. Electrochemical degradation of acid yellow 23 by anodic oxidation–optimization of operating parameters. J. Environ. Eng. (ASCE) 142, 5.
González, M., Arana, J., González, O., Herrera-Melián, J.A., Doña, J.M., Pérez, J.M., 2014. Detoxification of the herbicide propanil by means of Fenton process and TiO_2-photocatalysis. J. Photochem. Photobiol. A Chem. 291, 34–43.
He, R., Tian, B., Qi-Qi, Z., Hong-Tao, Z., 2015. Effect of Fenton oxidation on biodegradability, biotoxicity and dissolved organic matter distribution of concentrated landfill leachate derived from a membrane process. Waste Manag. 38, 232–239.
Kavitha, V., Ppanalivelu, K., 2005. Degradation of nitrophenols by Fenton and photo-Fenton processes. J. Photochem. Photobiol. A Chem. 170 (1), 83–95.
Khouni, I., Marrot, B., Moulin, P., Amar, R., 2011. Decolourization of the reconstituted textile effluent by different process treatments: enzymatic catalysis, coagulation/flocculation and nanofiltration processes. Desalination 268, 27–37.
Kwang-Ho, C., Sang-June, C., Eui-Deog, H., 2007. Effect of coagulant types on textile wastewater reclamation in a combined coagulation/ultrafiltration system. Desalination 202, 262–270.
Lapertot, M., Ebrahimi, S., Dazio, S., Rubinelli, A., Pulgarin, C., 2007. Photo-Fenton and biological integrated process for degradation of a mixture of pesticides. J. Photochem. Photobiol. A Chem. 186, 34–40.
Li, J., Zhao, L., Qin, L., Tian, X., Wang, A., Zhou, Y., Meng, L., Chen, Y., 2016. Removal of refractory organics in nanofiltration concentrates of municipal solid waste leachate treatment plants by combined Fenton oxidative-coagulation with photo e Fenton processes. Chemosphere 146, 442–449.
Malato, S., Fernández-Ibáñez, P., Maldonado, M.I., Blanco, J., Gernjak, W., 2009. Decontamination and disinfection of water by solar photocatalysis: recent overview and trends. Catal. Today 147, 1–59.
Miralles-Cuevas, S., Oller, I., Ruiz Aguirre, A., Sánchez Pérez, J.A., Malato, S., 2014. Removal of pharmaceuticals from MWTP effluent by nanofiltration and solar photo-Fenton using two different iron complexes at neutral pH. Water Res. 64, 23–31.
Montgomery, D.C., 2010. Design and Analysis of Experiments, 8 edition. Wiley. ISBN-13: 978–1118146927.
Moncayo-Lasso, A., Pulgarin, C., Benítez, N., 2008. Degradation of DBP's precursors in river water before and alter show filtration by photo-Fenton process at pH 5 in a solar CPC reactor. Water Res. 42, 4125–4132.
Nidheesh, P., Gandhimathi, R., Ramesh, S., 2013. Degradation of dyes from aqueous solution by Fenton processes: a review. Environ. Sci. Pollut. Res. 20, 2099–2132.
Papoutsakis, S., Miralles-Cuevas, S., Gondrexon, N., Baup, S., Malato, S., Pulgarin, C., 2015. Coupling between high-frequency ultrasound and solar photo-Fenton at pilot scale for the treatment of organic contaminants: an initial approach. Ultrason. Sonochem. 22, 527–534.
Parra, S., Sarria, V., Malato, S., 2000. Photochemical versus coupled photochemical–biological flow system for the treatment of two biorecalcitrant herbicides: metobromuron and isoproturon. Appl. Catal. B Environ. 2, 153–165.
Pignatello, J.J., Oliveros, E., Mackay, A., 2006. Advanced Oxidation Processes for organic contaminant destruction based on the Fenton reaction and related chemistry. Environ. Sci. Technol. 37, (3), 273–275.
Perdigón-Melón, J.A., Carbajo, J.B., Petre, A.L., Rosal, R., García-Calvo, E., 2010. Coagulation–Fenton coupled treatment for ecotoxicity reduction in highly polluted industrial wastewater. J. Hazard. Mater. 181, 127–132.
Punzi, M., Nilsson, F., Anbalagan, A., Svensson, B.M., Jönsson, K., Mattiasson, B., Jonstrup, M., 2015. Combined anaerobic–ozonation process for treatment of textile wastewater: removal of acute toxicity and mutagenicity. J. Hazard., Mater. 292, 52–60.
Rodríguez-Chueca, J., Amor, C., Fernandes, J.R., Tavares, P.B., Lucas, M.S., Peres, J.A., 2016. Treatment of crystallized-fruit wastewater by UV-A LED photo-Fenton and coagulation-flocculation. Chemosphere 145, 351–359.
Rodriguez, M., Sarria, V., Esplugas, S., Pulgarin, C., 2002. Photo-Fenton treatment of biorecalcitrant wastewater generated in textile activities: biodegradability of the phototreated solution. J. Photochem. Photobiol. A Chem. 151, 129–135.
Secula, M.S., Stan, C.S., Cojocaru, C., Cagnon, B., Cretescu, I., 2014. Multi-objective optimization of indigo carmine removal by an electrocoagulation/GAC coupling process in a batch reactor. Sep. Sci. Technol. 49 (6), 924–938.
Senn, A.M., Russo, Y.M., Litter, M.I., 2014. Treatment of wastewater from an alkaline cleaning solution by combined coagulation and photo-Fenton processes. Sep. Purif. Technol. 132, 552–560.
Soares, P., Batalha, M., Selene, M.A., Souza, S.A.G.U., Boaventura, R.R., Vilar, V.P., 2015. Enhancement of a solar photo-Fenton reaction with ferric-organic ligands for the treatment of acrylic-textile dyeing wastewater. J. Environ. Manag. 120–131.
Soares, P., Silva, T.C.V., Manenti, D., Souza, S.A.G.U., Boaventura, R.R., Vilar, V.P., 2013. Insights into real cotton-textile dyeing wastewater treatment using solar advanced oxidation processes. Environ. Sci. Pollut. Res. 1–14.
Vedrenne, M., Vasquez-Medrano, R., Prato-Garcia, D., Frontana-Uribe, B.A., Ibañez, J.G., 2012. Characterization and detoxification of a mature landfill leachate using a combined coagulation–flocculation/photo Fenton treatment. J. Hazard. Mater. 205– 206, 208–215.
Verma, A.K., Dash, R.R., Bhunia, P., 2012. A review on chemical coagulation/flocculation technologies for removal of colour from textile wastewaters. J. Environ. Manag. 93, 154–168.
Zapata, A., Velegraki, T., Sánchez-Pérez, J., Mantzavinos, D., Maldonado, M., Malato, S., 2009. Solar photo-Fenton treatment of pesticides in water: effect of iron concentration on degradation and assessment of ecotoxicity and biodegradability. Appl. Catal. B Environ. 88, 448–454.

Update

Journal of Environmental Management

Volume 203, Issue P1, 1 December 2017, Page 615

DOI: https://doi.org/10.1016/j.jenvman.2017.03.092

Journal of Environmental Management 203 (2017) 615

Contents lists available at ScienceDirect

Journal of Environmental Management

journal homepage: www.elsevier.com/locate/jenvman

Corrigendum

Corrigendum to 'Coagulation-flocculation sequential with Fenton or Photo-Fenton processes as an alternative for the industrial textile wastewater treatment' [J. Environ. Manag. 191 (2017) 189–197]

Edison GilPavas [a, *], Izabela Dobrosz-Gómez [b], Miguel Ángel Gómez-García [c]

[a] GIPAB: Grupo de Investigación en Procesos Ambientales, Departamento de Ingeniería de Procesos, Universidad EAFIT, Carrera 49 #7 sur 50, Medellín, Colombia

[b] Grupo de Investigación en Procesos Reactivos Intensificados con Separación y Materiales Avanzados - PRISMA, Departamento de Física y Química, Facultad de Ciencias Exactas y Naturales, Universidad Nacional de Colombia, Sede Manizales, Campus La Nubia, Km 9 Vía al Aeropuerto la Nubia, Apartado Aéreo 127, Manizales, Caldas, Colombia

[c] Grupo de Investigación en Procesos Reactivos Intensificados con Separación y Materiales Avanzados - PRISMA, Departamento de Ingeniería Química, Facultad de Ingeniería y Arquitectura, Universidad Nacional de Colombia, Sede Manizales, Campus La Nubia, Km 9 Vía al Aeropuerto la Nubia, Apartado Aéreo 127, Manizales, Caldas, Colombia

The authors regret that the printed version of this above-mentioned paper contained an error in the affiliation of one of the authors. The affiliation appears as:

Izabela Dobrosz-Gómez[b]

[b]Grupo de Investigación en Procesos Reactivos Intensificados con Separación y Materiales Avanzados - PRISMA, Departamento de Física y Química, Facultad de Ciencias Exactas y Naturales, Sede Manizales, Campus La Nubia, Km 9 Vía al Aeropuerto la Nubia, Apartado Aéreo 127, Manizales, Caldas, Colombia.

and it should be instead:

Izabela Dobrosz-Gómez[b]

[b]Grupo de Investigación en Procesos Reactivos Intensificados con Separación y Materiales Avanzados - PRISMA, Departamento de Física y Química, Facultad de Ciencias Exactas y Naturales, Universidad Nacional de Colombia, Sede Manizales, Campus La Nubia, Km 9 Vía al Aeropuerto la Nubia, Apartado Aéreo 127, Manizales, Caldas, Colombia.

The authors would like to apologise for any inconvenience caused.

DOI of original article: http://dx.doi.org/10.1016/j.jenvman.2017.01.015.

* Corresponding author.
E-mail address: egil@eafit.edu.co (E. GilPavas).

http://dx.doi.org/10.1016/j.jenvman.2017.03.092